# CONFORMATION AND ORIENTATION OF GRAMICIDIN A IN ORIENTED PHOSPHOLIPID BILAYERS MEASURED BY SOLID STATE CARBON-13 NMR

BRUCE A. CORNELL,* FRANCES SEPAROVIC,* ATTILIO J. BALDASSI,[‡] AND ROSS SMITH[‡]
*Commonwealth Scientific and Industrial Research Organization, Division of Food Research, North Ryde, New South Wales, Australia; and [‡]Department of Biochemistry, University of Queensland, St. Lucia, Queensland 4067, Australia

ABSTRACT    Three analogues of the helical ionophore gramicidin A have been synthesized with $^{13}$C-labeled carbonyls ($^{13}$C=O) incorporated at either $Gly^2$, $Ala^3$, or $Val^7$. A fourth compound incorporated $^{13}$C at both the carbonyl and α-carbon of $Gly^2$ within the same molecule. These labels were studied using solid-state, proton-enhanced, $^{13}$C nuclear magnetic resonance (NMR) in hydrated dispersions of dimyristoylphosphatidylcholine (DMPC)–gramicidin A. The dispersions were aligned on glass coverslips whose orientation to the magnetic field could be varied through 180°. The orientation dependence of the NMR spectrum was used to obtain an accurate measurement of the $^{13}$C chemical shift anisotropy (CSA), and in the case of the fourth compound, the $^{13}$C—$^{13}$C dipolar coupling constant. From the measured CSA and estimates of the orientation of the $^{13}$C shielding tensor, we are able to determine the direction of the $^{13}$C=O bonds and to compare these with the predictions of the various reported models for the configuration of gramicidin A in phospholipid bilayers. Our results are consistent with the left-handed $\pi\pi^{6.3}_{LD}$ single-stranded helix (Urry, D. W., J. T. Walker, and T. L. Trapane. 1982. *J. Membr. Biol.* 69:225–231). The right-handed $\pi\pi^{6.3}_{LD}$ single-stranded helix observed for gramicidin A in sodium dodecyl sulfate micelles (Arseniev, A. S., I. L. Barsukov, V. F. Bystrov, A. L. Loize, and Yu A. Ovchinnikov. 1985. *FEBS (Fed. Eur. Biochem. Soc.) Lett.* 186:168–174) yields a poorer fit to the data. However, the width of the carbonyl resonances suggests a distribution of molecular geometries possibly resulting from a spread in the helix pitch and handedness. Double-stranded helices and β sheet structures are excluded. In dispersions in which the lipid is in the $L_\alpha$ phase, the gramicidin A undergoes rapid reorientation about an axis which is centered on the normal to the plane of the coverslips. When the supporting lipid is in the $L_\beta$ phase the helices are rigid on the timescale of $^{13}$C-NMR. The configuration of gramicidin A is unaltered by $L_\alpha$-$L_\beta$ phase transition of the bilayer lipid.

## INTRODUCTION

Gramicidin A is a low molecular weight (1,882 mol wt) ionophore that selectively facilitates the transport of small monovalent cations across lipid bilayers. It is one of a family of linear polypeptides produced during active growth of the microorganism *Bacillus brevis* (Katz and Demain, 1977). Many research themes have emerged from the study of gramicidin A. Because of the volume of publications reporting on the properties and structure of gramicidin A only a representative list is given here. These include the energetics of ion transport across membranes (Hladky and Haydon, 1972; Monoi, 1983; Eisenman and Sandblom, 1984; Jordan, 1984; Mackay et al., 1984; Urry et al., 1984; Etchebest et al., 1985; Kim et al., 1985; Prasad et al., 1986); the effect of gramicidin A on the order, dynamics, and phase stability of the supporting lipid (Chapman et al., 1977; Rice and Oldfield, 1979; Haigh et

al., 1979; London and Feigenson, 1981; Rajan et al., 1981; Van Echteld et al., 1981; Cavatorta et al., 1982; Cornell and Keniry, 1983; Killian and de Kruijff, 1985 *a*, *b*; Tanaka and Freed, 1985; Killian et al., 1986); and the effect of environment on the secondary and tertiary structure of gramicidin A (Urry, 1971; Veatch and Blout, 1974; Bamberg et al., 1977; Koeppe et al., 1978; Weinstein et al., 1979, 1980, 1985; Wallace et al., 1981; Urry et al., 1982, 1983 *a*, *b*; Nabedryk et al., 1982; Sychev and Ivanov, 1982, 1984; Venkatachalam and Urry, 1983; Wallace, 1984, 1986; Naik and Krimm, 1984; Hawkes et al., 1984; Koeppe and Schoenborn, 1984; Arseniev et al., 1985 *a*, *b*). The combined results of this work have made gramicidin A one of the best understood examples of a transmembrane ion channel. Despite the extensive literature on gramicidin A its conformation in phospholipid bilayers remains uncertain.

In the present study we use cross-polarization $^{13}$C-nuclear magnetic resonance (NMR) to derive the orientation of the $^{13}$C=O bonds of the $Gly^2$, $Ala^3$, and $Val^7$

---

Address correspondence to B. A. Cornell.

residues of gramicidin A dispersed in aligned multilayers of dimyristoyl- and dimyristylphosphatidylcholine. From these bond directions and the molecular symmetry, it is possible to discount some of the structures that have been proposed for gramicidin A in phospholipid bilayers.

## MATERIALS AND METHODS

### Chemicals

Butyloxycarbonyl (BOC)-amino acids and BOC-trp-O-resin were purchased from Peninsular Laboratories, San Carlos, CA. 1-$^{13}$C-L-Alanine (90% enrichment) and 1-$^{13}$C-L-valine (99% enrichment) were obtained from the Commissariat a L'Energy Atomique (Saclay, France). 1,2-$^{13}$C-$C_2$-Glycine (90% enrichment) was obtained from Merck, Sharpe and Dohme Isotopes (Montreal, Canada), and 1-$^{13}$C glycine (90% enrichment) from KOR Isotopes (Cambridge, MA). Amino protection of the $^{13}$C amino acids was effected by addition of the butyloxycarbonyl group using di-$t$-butyl dicarbonate (Sigma Chemical Co., St Louis, MO) (Prasad et al., 1982) or BOC-ON (2-[tert-butoxycarbonyloxyamino]-2-phenylacetonitrile; Ega Chemie, Albuch, FDR), following the method of Itoh et al. (1975). Dimyristoylphosphatidylcholine (DMPC) was purchased from Calbiochem-Behring Corp., La Jolla, CA, and the chain perdeuterated analogue, dimyristolyphosphatidylcholine (d$_{54}$-DMPC) was purchased from Sedary Research Laboratories Inc., London, Ontario, Canada.

### Synthesis of $^{13}$C-labeled Peptides

Gramicidin A was synthesized using the solid-phase method, with minor variations from the procedure described by Prasad et al. (1982). The syntheses were performed manually starting with BOC-trp-resin (3.1 g containing 0.59 mequivalent tryptophan/g). Each amino acid was added with the following steps: (a) Resin washings with 3 × 30 ml $CH_2Cl_2$. (b) Removal of the protecting group in 30 ml 33% trifluoroacetic acid (Merck, Darmstadt, FDR), 5% ethanedithiol (Aldrich-Chemie, Steinheim, FDR), in $CH_2Cl_2$, containing 1% (wt/vol) indole (Sigma Chemical Co.). Two incubations were used, the first for 5 min and the second for 25 min. (c) Washings with 6 × 30 ml $CH_2Cl_2$. (d) Incubation for 5 min with two 30-ml aliquots of 5% (vol/vol) di-isopropylethylamine in dichloromethane. (e) Washings with 6 × 30 ml $CH_2Cl_2$. (f) Addition of the BOC-amino acid (see below). (g) Washings with 6 × 30 ml $CH_2Cl_2$.

After step (g) the extent of coupling was determined using a quantitative ninhydrin assay (Sarin et al., 1981).

The conditions used for coupling the amino acids varied. Initially a 2.5-fold excess of the BOC-amino acid in dimethylformamide (DMF) (BDH Chemicals, Poole, England) was added and stirred with the resin for 10 min. A 2.5-fold excess of dicyclohexylcarbodiimide (Protein Research Foundation, Osaka, Japan) in $CH_2Cl_2$ was then added and allowed to react at room temperature. For the first five to six cycles a 2-h incubation sufficed to give >99.8% reaction, however, for subsequent residue additions this incubation was extended to 4 h, and a second overnight coupling with a 1.5-fold excess of BOC-amino acid and dicyclohexylcarbodiimide was required. The $^{13}$C-labeled BOC-amino acids were added in equivalent molar amounts to the trp on the original resin, and allowed to react in the presence of dicyclohexylcarbodiimide overnight. This step was followed by a 4-h incubation with a 2.5-fold excess of the corresponding unlabeled BOC-amino acid.

The completed peptide was removed from the resin by reaction with ethanolamine, and formylated as described by Prasad et al., 1982. The crude gramicidin A was purified by filtration in methanol on a 100 cm × 3.2 cm diam column of Sephadex LH-20 (Pharmacia, Uppsala, Sweden). Fractions collected from this column were analyzed by high performance liquid chromatography on an analytical (8 mm internal diam × 10 cm), radial-compression column using an isocratic 83:17 (vol/vol) methanol/water solvent. Fractions containing predominantly material with the same HPLC retention time as the major peak from commercial gramicidin A

(Koch-Light, Colnbrook, England), were pooled. Further purification was achieved by preparative thin layer chromatography on 2-mm-thick silica gel plates (Merck Kieselgel 60 F-254). Bands visualized under short wavelength ultraviolet light were extracted from the resin using methanol, and analyzed by HPLC. The fractions containing the purest gramicidin were finally purified by repetition of the Sephadex LH-20 chromatography, or by preparative HPLC in 83:17 methanol/water, using the column described above, followed again by Sephadex LH-20 chromatography. The purity of the gramicidin was assessed to be >98% by HPLC, by 200 MHz $^1$H-NMR, and by thin layer chromatography (TLC) (silica gel G) with 85:15:3 $CHCl_3$/$CH_3CH_2OH$/acetone, as the ascending solvent. TLC spots were detected under UV radiation, or by charring with 25% $H_2SO_4$.

### Sample Preparation

Solutions of gramicidin A and DMPC (1:15 mol ratio) in $C_6H_6$/$CH_3CH_2OH$ (95:5) were pipetted onto the surface of typically, 50 microscope coverslips, each 15-mm long and a width chosen such that the stacked cross-section was circular with a diameter of <10 mm. The solvent was removed under vacuum overnight. The total weight of lipid plus gramicidin A was ~50 mg. Using a microliter syringe 2–5 μl of glass distilled water was added to the surface of each coverslip. The coverslips were stacked and the assembly sealed inside a 10-mm diam × 25-mm long NMR tube using a fine gas flame. Particular care was taken not to damage the dispersion. The sample was equilibrated for 2–3 h at 330 K and then cooled to the temperature at which the measurement was to be made. Longer periods of equilibration failed to improve the alignment of the oriented dispersions.

### NMR Spectroscopy

Spectra were acquired using a model CXP300 NMR spectrometer (Bruker Instruments, Inc., Billerica, MA). The NMR tube was mounted horizontally inside a four-turn, close-fitting, 18-gauge, silver-plated copper wire coil tuned to 75.46 MHz for $^{13}$C and 300.066 MHz for $^1$H. Spectra were obtained using the Pines et al. (1973) $^{13}$C, proton-enhanced, cross-polarization sequence. Typical operating conditions were: Hartmann-Hahn 90° pulse, 8 μs; repetition delay, 2 s; contact time, 1.5 ms; acquisition time 8.5 ms; sweep width, 60 kHz; 100,000 acquisitions per spectrum, obtained in lots of 10,000. The sample tube was mounted to permit rotation through an angular range of 180° about an axis perpendicular to the $B_o$ field. A goniometer built in this laboratory permitted the angle to be adjusted with the probe and sample in situ. The angle was calibrated from the $^1$H resonance "magic angle" effect. The reproducibility of the angle setting was ±1°. The water content of the sample was determined from the integrated $^1$H-NMR spectrum measured at the magic angle as shown in Fig. 1. The water content was checked before and after each period of acquisition. Owing to the slight (<1 K) heating effects of the radiofrequency (rf) field, a slow migration of water occurs from beneath the rf coil to the ends of the sample tube. If the water content was found to have changed significantly, the sample was re-equilibrated. The temperature rise due to rf heating was measured from the apparent depression of the phase transition temperature of a DMPC dispersion.

### Spectral Simulations

Spectral simulations were performed on a model HP1000F computer (Hewlett-Packard Co., Palo Alto, CA) using a frequency domain representation of the tensor distribution.

## RESULTS

### NMR of Dry Powders

Gramicidin A has the sequence HCO-L.Val$^1$-Gly$^2$-L.Ala$^3$-D.Leu$^4$-L.Ala$^5$-D.Val$^6$-L.Val$^7$-D.Val$^8$-L.Trp$^9$-
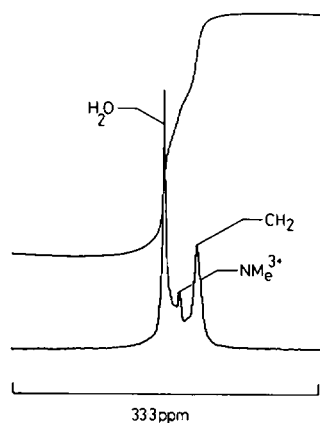
FIGURE 1 300 MHz $^1$H-NMR spectrum obtained from an aligned sample of gramicidin A and DMPC with the normal to the plane of the multilayers at the "magic angle" (54° 47') to the $B_o$ field. The resulting collapse of the dipolar interactions produces a separation of the $H_2O$, $NMe_3^+$ and aliphatic resonances of the sample. Spectrum simulation and comparison of the peak integrals provides a measure of the water content of the dispersion (typically 19–21 mol $H_2O$/mol DMPC). Acquisition parameters: sweep width, 10 kHz; 90° pulse duration, 7 $\mu$s; repetition delay, 10 s; 100 acquisitions; temperature, 300 K.

D.Leu$^{10}$-L.Trp$^{11}$-D.Leu$^{12}$-L.Trp$^{13}$-D.Leu$^{14}$-L.Trp$^{15}$-N HCH$_2$CH$_2$OH (Sarges and Witkop, 1965). Dry powders of the gramicidin A analogues with $^{13}$C=O at Gly$^2$, Ala$^3$, or Val$^7$, gave the spectra shown in Fig. 2. From these spectra we derived an average value for the principal shielding axes shown in the traceless form of $\sigma_{11} = -74 \pm 3$ ppm, $\sigma_{22} = -7 \pm 3$ ppm, and $\sigma_{33} = +82 \pm 3$ ppm. Within experimental precision the three analogues gave the same shielding tensor. The principal shielding values are close to those obtained from the dipeptide glycyl-glycine · HCl ·
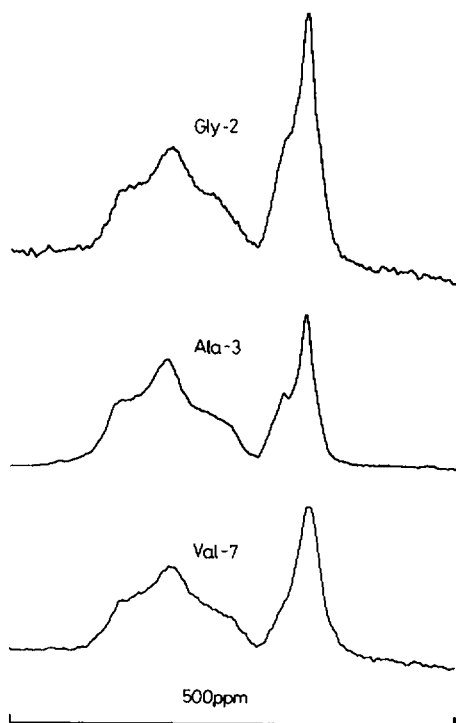


FIGURE 2 75 MHz $^{13}$C cross-polarization NMR spectra of dry powders of $^{13}$C-labeled analogues of gramicidin A with $^{13}$C=O groups at the residues of Gly$^2$, Ala$^3$, and Val$^7$. Acquisition parameters: sweep width, 62.5 kHz; 90° spin-locking pulse duration, 4 $\mu$s; Hartmann-Hahn contact time, 1 ms; repetition delay, 1 s; broadening, 50 Hz; 10,000 acquisitions; temperature, 273 K.

$H_2O$ (Stark et al., 1983). Magic angle spinning of dry powdered Ala$^3$-labeled gramicidin A revealed that ~ 90% of the total spectrum intensity in the low field region of Fig. 2 arose from the carbonyl resonances of the polypeptide backbone.

## NMR of Hydrated Dispersions with d$_{54}$-DMPC

Incorporation of the Val$^7$ gramicidin A analogue (1:15) into multilamellar dispersions of chain perdeuterated DMPC (d$_{54}$-DMPC) yields the spectra shown in Fig. 3 (Smith and Cornell, 1986). The d$_{54}$-DMPC analogue of DMPC minimizes the contribution to the cross-polarization $^{13}$C spectrum of the lipid. Despite the major reduction in the CH$_2$ peak in Fig. 3 the d$_{54}$-DMPC carbonyl resonance is only halved in intensity. This indicates that at least half the cross-polarization of the lipid carbonyl groups is derived from the glycerol protons. At temperatures well below the L$_\beta$-P$_{\beta'}$ phase boundary the carbonyl resonance from the lipid–gramicidin A dispersion indicates a rigid structure. When the temperature is raised to 5° below the d$_{54}$-DMPC main transition temperature (~290 K at this hydration), the carbonyl resonance narrows, indicating the onset of motion by the gramicidin A. As seen from the d$_{54}$-DMPC methylene resonance, the lipid has yet to undergo the transition to a fluid state. By 289 K the gramicidin A carbonyl resonance has reached a limiting width while the d$_{54}$-DMPC methylene resonance reflects a mixed phase. At 297 K the d$_{54}$-DMPC has fully undergone the main phase transition and peaks due to the d$_{54}$-DMPC carbonyls are superimposed on the carbonyl peak from the gramicidin A. Similar results were obtained for the Gly$^2$- and Ala$^3$-labeled compounds.
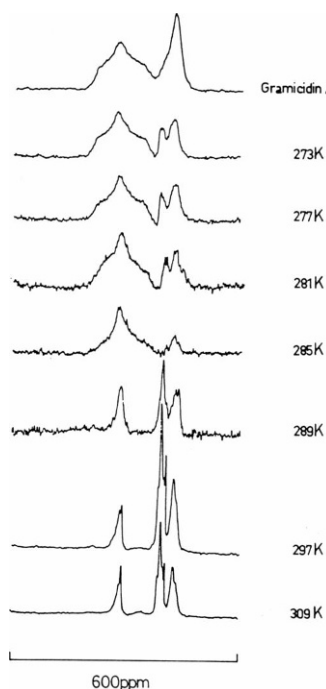


FIGURE 3 75 MHz $^{13}$C cross-polarization NMR spectra of the Val$^7$-labeled analogue of gramicidin A in a hydrated disperson of perdeuterated d$_{54}$-DMPC at a mole ratio of 1:15. A temperature independent spectral component thought to be undispersed gramicidin A and amounting to ~20% of the signal intensity was subtracted. Acquisition parameters: sweep width, 62.5 kHz; 90° spin locking pulse duration, 5 $\mu$s; Hartmann-Hahn contact time, 1 ms below and 2 ms above the main transition temperature; repetition delay, 2 s. The temperature at which each spectrum was acquired is shown adjacent to each curve.
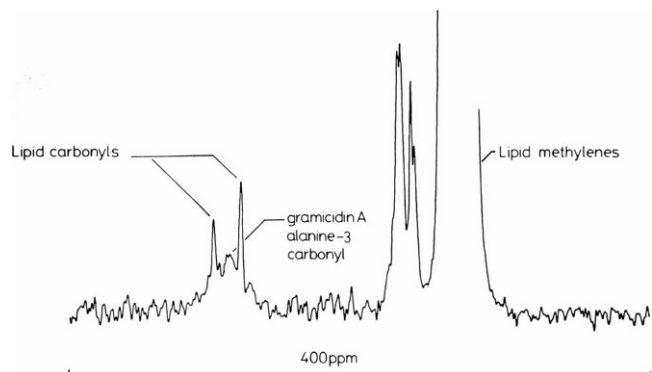
FIGURE 4    75 MHz $^{13}$C cross-polarization NMR spectrum of the Ala$^3$-labeled analogue of gramicidin A dispersed with hydrated multilayers of DMPC (1:15 mol ratio) and aligned on a stack of 50 microscope coverslips. The normal to the plane of the multilayers was directed along the B$_o$ field (0° orientation). Acquisition parameters: sweep width, 62.5 kHz; 90° spin locking duration, 9 μs; Hartmann-Hahn contact time, 2 ms; repetition delay, 2 s; line broadening, 50 Hz; 23,000 acquisitions; temperature, 308 K.

## NMR of Aligned Dispersions with d$_{54}$-DMPC and DMPC

*High Temperature Phase.*   The $^{13}$C spectrum of the Ala$^3$ analogue aligned in DMPC at 307 K is shown in Fig. 4. The sample is oriented with the slide normal parallel to the B$_o$ field (0° orientation). The unresolved carbonyl multiplet seen at high temperatures in Fig. 3 is now separated into two narrow lipid peaks and a broader gramicidin A resonance. The dependence on orientation of these three signals is shown in Fig. 5. The gramicidin A
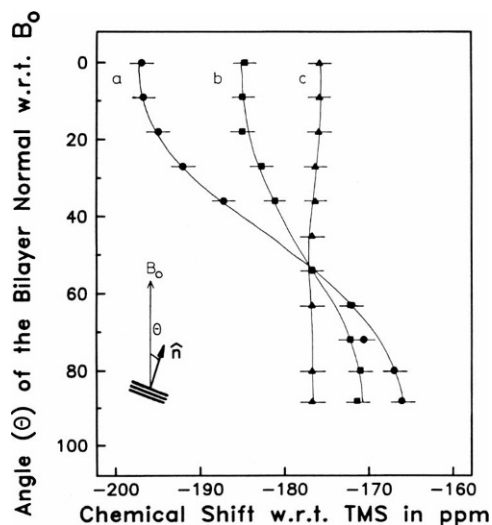


FIGURE 5    Dependence of the resonance position of the three carbonyl peaks seen in Fig. 4, on the orientation angle θ between the normal to the plane of the coverslips and the B$_o$ field. The CSA of (*a*) the DMPC sn-1 chain ester carbonyl (−30 ± 1 ppm), (*b*) the Ala$^3$-labeled analogue of gramicidin A (−16 ± 1 ppm), and (*c*) the DMPC sn-2 chain ester carbonyl (+2 ± 1 ppm).

carbonyl chemical shift anisotropy (CSA) may now be measured as −16 ppm. Fig. 6 shows the carbonyl regions at orientations with the normal to the slide at 0°, the "magic angle" and 90° relative to the B$_o$ field. Lorentzian simulations of the peaks and the de-convoluted contribution of the gramicidin A are shown adjacent to each spectrum. The half height peak width of the gramicidin A $^{13}$C=O resonance of 1,900 ± 150 Hz is constant from 0° to the "magic angle" but falls to 900 ± 150 Hz at 90°. Similar results were obtained for the Val$^7$ analogue. Aligned dispersions containing the even numbered Gly$^2$ analogue have a $^{13}$C=O CSA of −9 ppm. Examples of the spectrum at 0° orientation for the single labeled analogues are shown in Fig. 7. The lipid carbonyl resonances from the Val$^7$ analogue are smaller than that from the other dispersions owing to the use of d$_{54}$-DMPC. The use of d$_{54}$-DMPC did not prevent the sn-2 lipid carbonyl peak obscuring the signal from the Gly$^2$ analogue, making it difficult to obtain an accurate estimate of the CSA. In Fig. 8 we show that the $^{13}$C=O peak of the Gly$^2$ analogue may be resolved by using ether-linked lipids. The ester carbonyl resonance from the lipid is lost and an additional peak is evident in the glycerocholine region of the spectrum due to the ether methylene carbon. Use of ether-linked lipids permits a comparison of the spectrum of the single and double $^{13}$C-labeled Gly$^2$ analogue. As seen in Fig. 9 the dipolar interaction of the alpha and carbonyl carbons produce a doublet with a splitting of 1,900 ± 150 Hz.
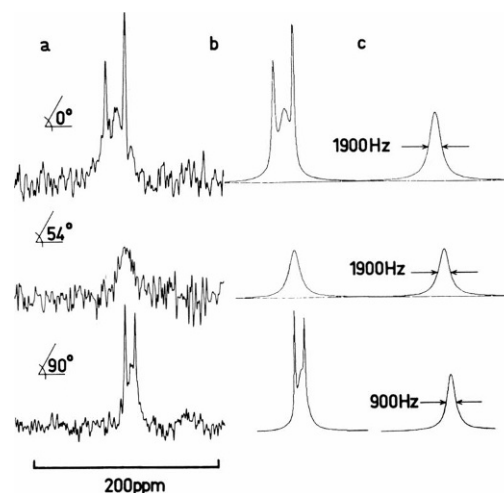


FIGURE 6    (*a*) Carbonyl region of the 75 MHz, $^{13}$C cross-polarization NMR spectrum of Ala$^3$-labeled gramicidin A analogue in an aligned, hydrated disperson of DMPC. The normal to the plane of the multilayers was oriented at 0°, the "magic angle" (54° 47′), and 90° to the B$_o$ field. Acquisition parameters: sweep width, 62.5 kHz; 90° spin locking pulse duration, 8 μs; Hartmann-Hahn contact time, 2 ms; repetition delay, 2 s; line broadening, 50 Hz; 60,000 (0°), 100,000 ("magic angle"), and 70,000 (90°) acquisitions; temperature, 308 K. (*b*) Lorentzian simulations from which it was possible to deconvolute the contribution of the gramicidin A $^{13}$C=O groups. (*c*) The deconvoluted spectra from the gramicidin A $^{13}$C=O groups. The line widths at 0°, "magic angle" and 90° were 1,900 ± 150, 1,900 ± 150, and 900 ± 150 Hz, respectively.
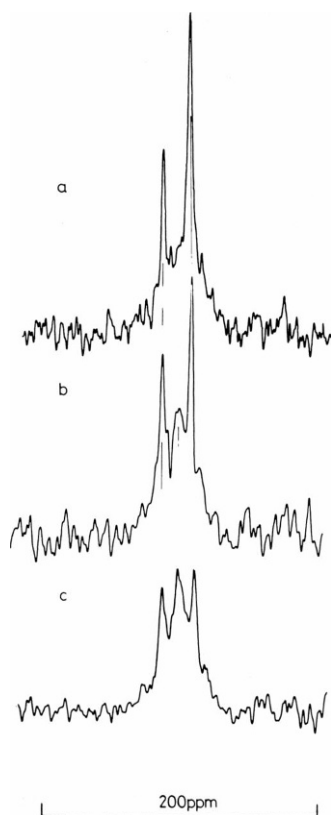
FIGURE 7 Comparison of the 0° orientation of gramicidin A analogues dispersed in DMPC (1:15) with $^{13}C{=}O$ labels at (a) $Gly^2$, (b) $Ala^3$, and (c) $Val^7$. Whereas the sn-1 and sn-2 carbonyl peaks from the lipid are well resolved from $Val^7$ and $Ala^3$ carbonyl resonances, the $Gly^2$ carbonyl peak is obscured. The acquisition parameters were similar to those in Figs. 4 and 6 for the 0° orientation; temperature, 308 K.

200ppm



500 ppm

FIGURE 8 Comparison of the 75 MHz, $^{13}C$ cross-polarization NMR spectra of the $Gly^2$-labeled gramicidin A analogue dispersed in either (a) hydrated dimyristoyl (ester-linked chains) or (b) dimyristyl (ether-linked chains) phosphatidylcholine, at a mole ratio of 1:15. The dispersions were aligned with the normal to the multilayers along the $B_0$ field. The arrow in spectrum b denotes the peak arising from the methylene carbon adjacent to the ether oxygen. The inset in a has a larger vertical gain by a factor of 1.5. Acquisition parameters: sweep width 62.5 kHz; 90° spin locking duration, 7 $\mu s$; Hartmann-Hahn contact time, 1.5 ms; repetition delay, 2 s; line broadening, 50 Hz; 30,000 acquisitions; temperature, 308 K.

## Low Temperature Phase

Cooling the aligned dispersion to 274 K causes no change in the shape or position of the gramicidin A carbonyl spectra obtained from samples at the 0° orientation. An example of this is seen in a comparison of the high and low temperature 0° orientations for the $Gly^2$ analogue, shown in Figs. 8 and 10. From Fig. 10 it is evident that the behavior of the spectrum at other orientations is very different when the sample is cooled such that the lipid is in the $L_{\beta'}$ phase. The peak broadens substantially as the angle of the slide normal approaches 90° to the $B_0$ field. At 308 K with the lipid in the $L_\alpha$ phase the same change in angle primarily causes a shift in position and an approximately twofold reduction in peak width. Simulations of these effects are given in a following section.

## DISCUSSION

The configuration of gramicidin A has been shown to depend upon its environment. In dioxane solution two forms exist. One of these, termed species 3, is a $\downarrow\uparrow\pi\pi^{5.6}{}_{LD}$ antiparallel left-handed, double-stranded helical dimer. The other, species 4 is a $\uparrow\uparrow\pi\pi^{5.6}{}_{LD}$ parallel right-handed, double-stranded helical dimer (Veatch et al., 1974; Sychev et al., 1980; Arseniev et al., 1984). In sodium dodecyl sulfate (SDS) micelles, gramicidin A forms a single-stranded $\overrightarrow{\pi}\overleftarrow{\pi}^{6.3}{}_{LD}$ head-to-head, right-handed, helical dimer (Arseniev et al., 1985b). In dispersions of lysophos-phatidyl-choline, it has been shown that a single-stranded
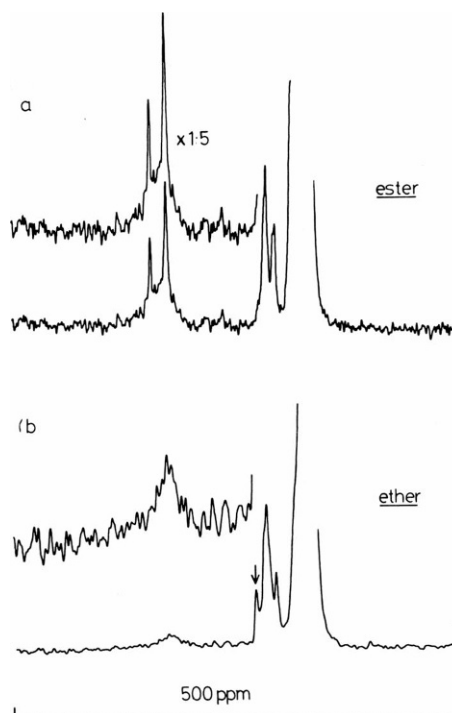
$\overrightarrow{\pi}\overleftarrow{\pi}^{6.3}{}_{LD}$ head-to-head, left-handed, helical dimer is formed (Urry et al., 1982, 1983a, b). When complexed with cesium ions and dissolved in a methanol-chloroform solution yet another structure is found (Arseniev et al., 1985a). This is a double-stranded $\downarrow\uparrow\pi\pi^{7.2}{}_{LD}$ antiparallel right-handed double helical dimer. Many techniques, including, infra-red, fluorescence and circular dichroism spectroscopy (Veatch et al., 1974; Veatch and Blout, 1974; Sychev et al., 1980; Wallace et al., 1981; Nabedryk et al., 1982; Urry et al., 1983a, b; Cavatorta et al., 1982; Sychev and Ivanov, 1984; Naik and Krimm, 1984; Wallace, 1984, 1986; Urry, 1984), solution NMR (Fossel et al., 1974; Urry et al., 1979, 1982; Weinstein et al., 1979, 1980, 1985; Arseniev et al., 1984, 1985a, b; Hawkes et al., 1984), and x-ray (Koeppe et al., 1978; Kimball and Wallace, 1984; Wallace, 1986) and neutron diffraction (Koeppe and Schoenborn, 1984) have been used to probe the conformation of gramicidin A. Yet none of these approaches has provided a unique conformation for gramicidin A in phospholipid bilayers. The structural detail available through the use of high resolution NMR techniques is overshadowed by the need to use an isotropic solvent system.
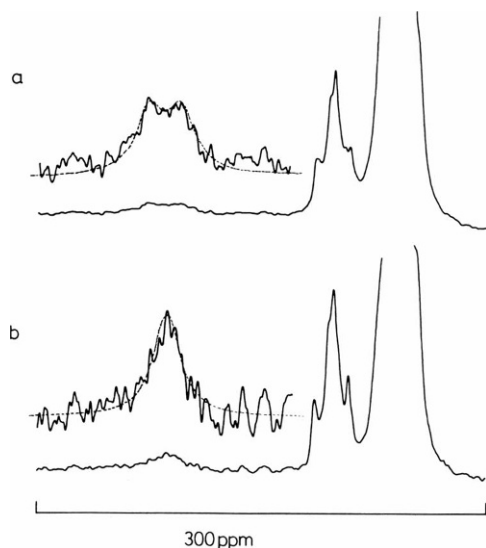
FIGURE 9  Comparison of the 75 MHz, $^{13}$C cross-polarization NMR spectra of an aligned, hydrated dimyristylphosphatidylcholine (ether linked) dispersion of the Gly$^2$-labeled gramicidin A analogue, (1:15) with the spectrum from a similar dispersion containing the double-labeled Gly$^2$ ($^{13}$C=O, $^{13}$C$_\alpha$-carbon) analogue. The normal to the multilayers was oriented along the B$_o$ field. The spectra are superimposed on Lorentzian functions which, for the single-labeled compound is a single Lorentzian with a full width half-height of 1,900 Hz, and for the double-labeled compound is two Lorentzians of the same width but a separation of 1,900 Hz. The insets in the carbonyl region of the spectrum have an eightfold increase in the vertical scale. Acquisition parameters: sweep width, 62.5 kHz; 90° spin locking pulse, 7 μs; Hartmann-Hahn contact time, 1.5 ms; repetition delay, 2 s; line broadening, 50 Hz; 150,000 (double label) and 50,000 (single label) acquisitions; temperature, 308 K.



FIGURE 10  75 MHz $^{13}$C cross-polarization NMR spectra of the Gly$^2$ labeled analogue of gramicidin A dispersed (1:15) with aligned DMPC multilayers in the L$_\beta$ phase at 274 K, and orientations of the multilayer normal at 0°, 25°, 45°, 60°, and 90° to the B$_o$ field. The rigid powder pattern of the Gly$^2$ labeled analogue is redrawn from Fig. 2. Acquisition parameters: sweep width, 62.5 kHz; 90° spin locking time, 6 μs; Hartmann-Hahn contact time, 1 ms; repetition delay, 1 s; line broadening, 50 Hz; typically 100,000–180,000 acquisitions.

Techniques such as infrared or circular dichroism spectroscopy are currently limited to providing a "fingerprint" of the class of structure adopted by the gramicidin A. X-ray and neutron diffraction require single crystals that may possess a different molecular geometry to the dispersion structure. For example, it has been found that the structure of the cesium complex determined by x-ray diffraction is different from that of gramicidin A in dispersions with phospholipid (Wallace, 1986). Furthermore, it has been shown to possess an opposite handedness to gramicidin A–cesium complex dissolved in chloroform-methanol (Arseniev et al., 1985a).

Despite the absence of direct evidence, a combination of techniques has produced a highly constraining set of requirements to which any model for the configuration of gramicidin A in phospholipid bilayers must comply. To date, three types of structure have been proposed. These are the parallel and antiparallel double-stranded helical dimers (Veatch et al., 1974; Arseniev et al., 1984), the end-to-end, single-stranded helical dimers (Urry et al., 1982, 1983), and aggregates of β sheet (Sychev and Ivanov, 1982, 1984).

We have used $^{13}$C-NMR of gramicidin A in aligned phospholipid bilayers to measure the bond directions of representative carbonyl groups. A starting point for our
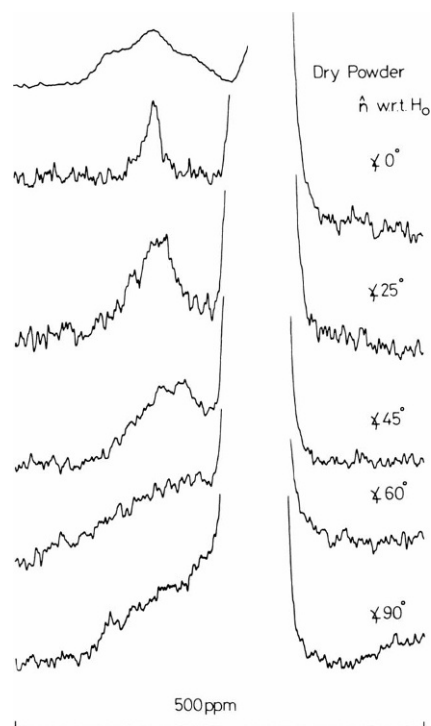
analysis is to note that when the aligned dispersions are cooled and the gross molecular motion eliminated, the carbonyl spectra at the 0° orientation are unaltered. This indicates that the polypeptide has a symmetry axis directed along the bilayer normal. This result also demonstrates the absence of substantial fluctuations in the alignment of gramicidin A relative to the plane of the bilayer or in its internal geometry. This does not exclude small amplitude bond vibrations that may be independent of the compressibility of the surrounding lipid. A recent deuterium NMR study by Datema et al., 1986, has observed the onset of axial rotation by gramicidin A on heating through the lipid phase transition.

Treating gramicidin A as either a rigid sheet or cylinder we may test the predicted CSA of the current models against the experimental NMR data. Figs. 11–13 show the direction of the peptide carbonyl bonds relative to the symmetry axis appropriate to each model. The helix axis is taken as the symmetry axis in both the single- and double-stranded helix models. For the β sheet aggregates, we have taken the long axis of the "J-hairpin" (Sychev and Ivanov, 1982) as the symmetry axis. As seen in Fig. 11 there is a common orientation for all of the carbonyl bonds in the β sheet aggregate. In the helical structures, the carbonyl
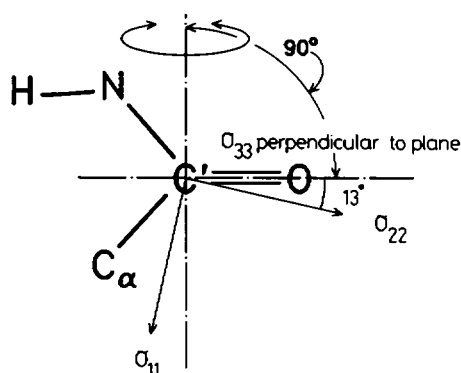
FIGURE 11 Common orientation of all amide carbonyl bonds relative to the long axis of the "J" hairpin structure, proposed (Sychev and Ivanov, 1982) for gramicidin A.



FIGURE 13 Orientation of type A and type B sites relative to the helix axis for the single-stranded $\pi\pi^{6.3}{}_{LD}$ helix proposed (Urry et al., 1982, 1983) for gramicidin A. The assignment of the sites to the odd or even amino acid residues depends on the details of the helix (see text).

bond direction depends upon whether the amino acid is an odd- or even-numbered residue. Fig. 12 shows the two sites found in the parallel and antiparallel double-stranded $\pi\pi_{LD}$ helices, and Fig. 13 the two sites for the single-stranded $\pi\pi_{LD}$ helices. The predicted CSA for each of these structures assuming rapid reorientational averaging about the symmetry axis is given in Table I. These predictions are contrasted with the measured values from the three analogues in dispersions at 308 K with the lipid in the $L_\alpha$ phase. The double-stranded helices and the $\beta$ sheet configurations fail to predict the experimental CSA. The data are best matched by assigning the Gly² label to type B site and the Ala³ and Val⁷ labels to the type A site of a single-stranded left-handed $\vec{\pi}\,\vec{\pi}^{6.3}{}_{LD}$ helix. Agreement with the single-stranded right-handed $\vec{\pi}\,\vec{\pi}^{6.3}{}_{LD}$ helix requires the reversal of the assignment of the type A and B sites. The difference in direction of the carbonyl bonds between these two cases is only 15°. Given the uncertainty in the detailed

conformation of these structures and the uncertainty in the orientation of the ¹³C shielding tensor (typically ±5°) we are reluctant to exclude the latter geometry. Further support for this general interpretation was obtained from the double-labeled Gly² analogue of gramicidin A. The residual dipolar coupling for the ¹³C—¹³C interaction between the alpha and carbonyl carbons is shown in Table II for a selection of geometries. Again, the single-stranded, left-handed $\vec{\pi}\,\vec{\pi}_{LD}$ helix is consistent with the measured data. The disorder of the symmetry axis is also seen to be small with a simple axial reorientation accounting for the reduced dipolar coupling. In total there are four single-stranded $\vec{\pi}\,\vec{\pi}^{6.3}{}_{LD}$ helices which may need to be considered. In the left-handed helix described by Urry et al., 1980, the type A sites are associated with the odd-numbered residues and the type B sites with the even-numbered residues. In the right-handed helix described by Arseniev et al., 1985, the assignment is reversed. Two more single-stranded helices may be generated by reversing the helix handedness while maintaining the assignment of the type A and B sites as before. However, from wire models of these structures, they may be energetically unfavorable due to the steric
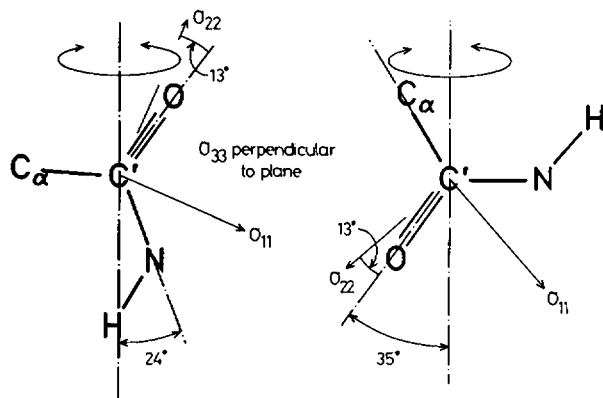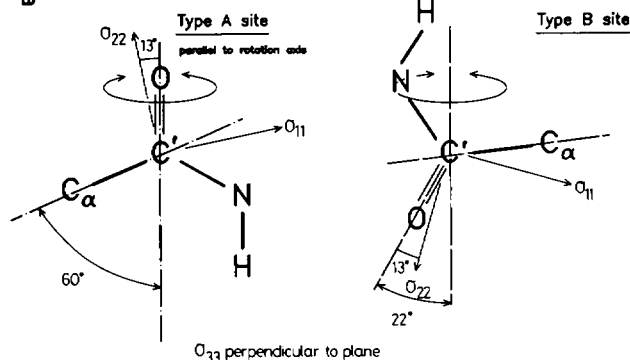


FIGURE 12 Orientation of type A and type B carbonyl sites relative to the helix axis for the double-stranded $\pi\pi^{5.6}{}_{LD}$ helix proposed (Veatch et al., 1974; Sychev et al., 1980; Arseniev et al., 1984) for gramicidin A. The assignment of the sites to odd- or even-numbered amino acid residues depends on the details of the helix (see text).

TABLE I

THE PREDICTED RESIDUAL CSA FOR THE ¹³C = O RESONANCE IN A LABELED ANALOGUE OF GRAMICIDIN A WHICH IS RAPIDLY REORIENTING ABOUT THE SYMMETRY AXIS APPROPRIATE TO EACH STRUCTURE

| Structure | CSA | |
|---|---|---|
| $\beta$ sheet | −102 ppm | |
| $\pi\pi^{5.6}{}_{LD}$ | −26 ppm (Type A) | −65 ppm (Type B) |
| $\pi\pi^{6.3}{}_{LD}$ | −17 ppm (Type A) | −13 ppm (Type B) |
| Experimental result | −16 ± 1 ppm (Ala³, Val⁷) | −9 ± 1 ppm (Gly²) |

The orientation and magnitude of the ¹³C = O tensor was taken from Stark et al., 1983, as −74 ppm, −7 ppm, and 82 ppm, for $\sigma_{11}, \sigma_{22}$, and $\sigma_{33}$, respectively, with $\sigma_{33}$ perpendicular to the plane of the O-C = O group and $\sigma_{22}$ tilted by 13° from the C = O bond direction.

| Structure | Dipolar splitting at 0° orientation | |
|---|---|---|
| $\beta$ sheet | 2,375 Hz | |
| $\pi\pi^{5,6}_{LD}$ | 1,830 Hz (Type A) | 2,860 Hz (Type B) |
| $\pi\pi^{6,3}_{LD}$ | 475 Hz (Type A) | 1,857 Hz (Type B) |
| Experimental result | 1,900 ± 150 Hz | |

The dipolar coupling constant was calculated from $\gamma_i/r^{-3}$ as 2,087 Hz using a C-C bond distance of 0.1540 nm. The 90° discontinuities in the $^{13}C$ powder pattern of the double labeled glycine from which the labeled gramicidin A was synthesized had a separation of 1,900 Hz.

interference of some of the amino acid side chains with the polypeptide backbone. The angular dependence seen for the dispersions in the fluid phase excludes macroscopic aggregation of the gramicidin A. However, aggregates on the molecular scale could reorient sufficiently rapidly to give the observed axially symmetric spectra.

A result that requires further explanation is the width of the peaks seen in Figs. 8 and 10 for the 0° orientation. As this width does not alter on freezing of the lipid, it is unlikely to be dominated by either relaxation effects or by a slow dynamic disorder. For the same reason we discount dipolar coupling to the amide $^{14}N$. Mosaic spread of the sample alignment is unlikely to be the mechanism. An intrinsic check of the bilayer mosiac spread is available in the lipid linewidth, which is five to six times narrower than that from the gramicidin at all angles.

It should be noted that the carbonyl signal from the gramicidin-containing dispersion at the "magic angle" (Fig. 6) is two to three times less intense than at 0°, and could arise from nonaligned material normally not visible. The nonaligned lipid peaks are weak at the contact time of 2 ms used to obtain these spectra.

A measurement of the $^{13}C$ $T_2$ at the 0° orientation of the Ala$^3$ analogue gave 700 ± 100 $\mu$s. This accounts for less than one-third of the linewidth of the gramicidin A carbonyl peaks and eliminates relaxation as the major cause of the broad carbonyl resonance from the gramicidin.

One possible source of the linebroadening is a distribution of molecular geometry within the gramicidin A. This may include minor changes in the number of residues per turn or even the handedness of the helix. The direction of the carbonyl bonds change by only 22° with a change in the handedness of the helix. The free energy difference between the left- and right-handed configurations is ~2 kcal/mol (Venkatachalam and Urry, 1983). A recent study by Weinstein et al., 1985, has reported a configurational heterogeneity for a series of $^{19}F$-labeled gramicidin A analogues dispersed in DPMC vesicles. Although these authors concluded that the accessibility of these labels was

only consistent with the head-to-head, single-stranded $\overrightarrow{\pi} \overleftarrow{\pi}_{LD}$ helix structure for gramicidin A, they obtained two chemical shifts for the C-terminal fluorine labels on the outer leaflet of the DMPC vesicle. The origin of this effect may reflect the same structural heterogeneity seen in the present results.

One test of the proposed model of configurational heterogeneity is to observe the dependence of the lineshape on the slide orientation when the gramicidin A is rigid (Fig. 10). Simulations based on an arbitrary gaussian variation in the $^{13}C$=O bond direction (SD = 10°) are given in Figs. 14 and 15. The agreement with the experimental results seen in Fig. 10 is encouraging. The model also accounts for the lineshapes at the 0° and 90° orientations when the lipid is in the $L_\alpha$ phase (Fig. 5). At the 90° orientation in the $L_{\beta'}$ phase the greatly increased width of the spectrum from the aligned component reduces the signal intensity to a level that is similar to that of the powder signal. From Fig. 15 it is apparent that in the $L_{\beta'}$ phase only ~70% of the gramicidin A is well aligned.

The spectra shown in Fig. 14 are insensitive to the details of the heterogeneity and refinement of this model awaits the results obtained from other labeled analogues.
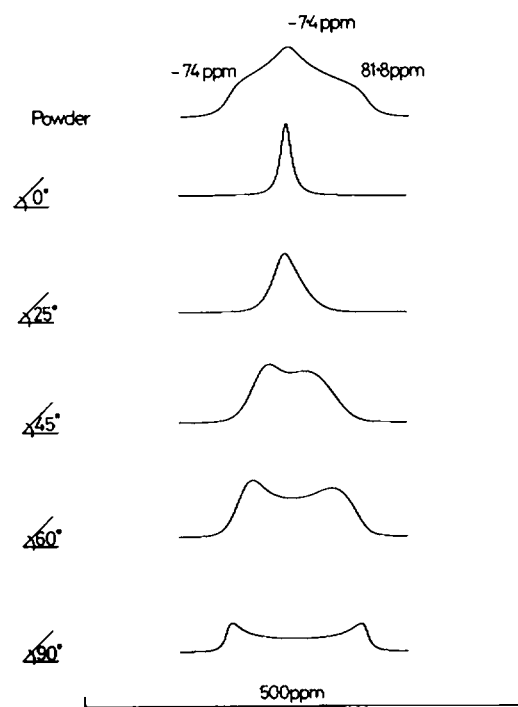


FIGURE 14 Computer generated simulations of the Gly$^2$-labeled gramicidin A dispersion in which the gramicidin A molecules are rigid, although aligned with the helix axis perpendicular to the plane of the multilayers. The orientation and amplitude of the CSA tensor was taken from Stark et al., 1983, with $\sigma_{22}$ 13° off the C=O bond direction and $\sigma_{33}$ perpendicular to the plane of the peptide bond. The simulation includes a gaussian (SD = 10°) distribution of the C=O bond direction and a Lorentzian linebroadening equivalent to a $T_2$ of 700 $\mu$s. The scale and angles have been chosen to allow easy comparison with the data in Fig. 10.
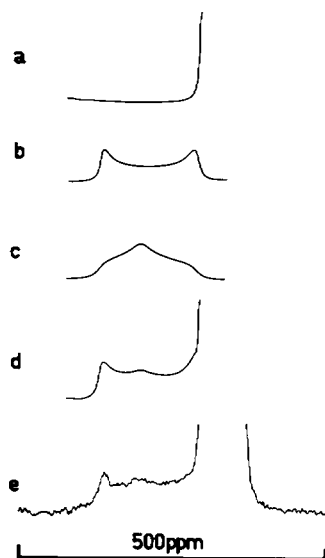
74

Figure 15 Computer simulations of a 75 MHz, $^{13}$C cross-polarization NMR spectrum of Ala$^3$-labeled gramicidin A analogue in an aligned, hydrated dispersion of DMPC at 274 K. The normal to the plane of the multilayers was oriented at 90° to the B$_0$ field. The simulation is compared with an experimental spectrum obtained using the conditions given in the caption to Fig. 10. Contributions are included from (a) the lipid methylene chains, (b) the aligned Ala$^3$-labeled gramicidin A carbonyls, and (c) the nonaligned Ala$^3$-labeled gramicidin A carbonyls. (d) Simulation generated from 1.5× (a) + 1.0× (b) + 0.5× (c). (e) Experimental spectrum.

The present study of the carbonyl bonds has emphasized the whole molecular motion of gramicidin A. In future reports we will address the orientation of the side chains and the effect of ions on the carbonyl bond directions.

## CONCLUSION

The results of this study permit us to make the following observations of a 1:15 gramicidin A per DMPC dispersion: (a) that gramicidin A intercalates into multilayers of DMPC with a geometry in which the carbonyl bond directions are broadly consistent with a $\vec{\pi}$ $\vec{\pi}^{6.3}$$_{LD}$ helix. The presence of what we interpret as a significant spread in direction about the mean suggests that the helices may possess both left- and right-handedness or a variation in pitch. The double-stranded helices and $\beta$ sheet structures are excluded. (b) When the DMPC is in the L$_\alpha$ phase the gramicidin A reorients about the long axis of the helix at a rate that exceeds the CSA (at 75 MHz) of ~14,000 s$^{-1}$. (c) When the DMPC is cooled to the L$_\beta$ phase the gramicidin A becomes rigid although its internal configuration and alignment relative to the bilayer remains unaltered. (d) On heating, motion of the gramicidin A is observed before the main transition temperature of the DMPC.

## REFERENCES

Arseniev, A. S., V. F. Bystrov, V. T. Ivanov, and Yu. A. Ovchinnikov. 1984. NMR Solution conformation of gramicidin A double helix. FEBS (Fed. Eur. Biochem. Soc.) Lett. 165:51–56.

Arseniev, A. S., I. L. Barsukov, and V. F. Bystrov. 1985a. NMR solution structure of gramicidin A complex with caesium cations. FEBS (Fed. Eur. Biochem. Soc.) Lett. 180:33–39.

Arseniev, A. S., I. L. Barsukov, V. F. Bystrov, A. L. Lomize, and Yu. A. Ovchinnikov. 1985b. $^1$H-NMR study of gramicidin A transmembrane ion channel. Head-to-head right-handed, single-stranded helices. FEBS (Fed. Eur. Biochem. Soc.) Lett. 186:168–174.

Bamberg, E., H. J. Apell, and H. Alpes. 1977. Structure of gramicidin A channel: discrimination between the $\pi_{LD}$ and the $\beta$ helix by electrical measurements with lipid bilayer membranes. Proc. Natl. Acad. Sci. USA. 74:2402–2406.

Cavatorta, P., A. Spisni, E. Casali, L. Linder, L. Masotti, and D. Urry. 1982. Intermolecular interactions of gramicidin A' channels incorporated into lysolecithin lipid systems. Biochim. Biophys. Acta. 689:113–120.

Chapman, D., B. A. Cornell, A. W. Eliasz, and A. Perry. 1977. Interactions of helical polypeptide segments which span the hydrocarbon region of lipid bilayers. Studies of the gramicidin A lipid-water system. J. Mol. Biol. 113:517–538.

Cornell, B. A., and M. A. Keniry. 1983. A proton enhanced carbon-13 NMR study of the effect of cholesterol and gramicidin A on the dynamics of phospholipid bilayers. Biochim. Biophys. Acta. 732:705–710.

Datema, K. P., K. P. Pauls, and M. Bloom. 1986. Deuterium nuclear magnetic resonance investigation of the exchangeable sites on gramicidin A and gramicidin S in multilamellar vesicles of dipalmitoylphosphatidylcholine. Biochemistry. 25:3796–3803.

Eisenman, G., and J. P. Sandblom. 1984. Modeling the gramicidin channel: interpretation of experimental data using rate theory. Biophys. J. 45:88–90.

Etchebest, C., A. Pullman, and S. Raganathan. 1985. The gramicidin A channel: theoretical energy profile computed for a single occupancy by a divalent cation, Ca$^{2+}$. Biochim. Biophys. Acta. 818:23–30.

Fossel, E. T., W. R. Veatch, Yu. A. Ovchinnikov, and E. R. Blout. 1974. A $^{13}$C nuclear magnetic resonance study of gramicidin A in monomer and dimer forms. Biochemistry. 13:5264–5275.

Haigh, E. A., K. R. Thulborn, and W. H. Sawyer. 1979. Comparison of fluorescence energy transfer and quenching methods to establish the position and orientation of components within the transverse plane of the lipid bilayer. Application to the gramicidin A bilayer interaction. Biochemistry. 18:3525–3532.

Hawkes, G. E., L. Y. Lian, and E. Randell. 1984. Conformational analysis of gramicidin A by $^{15}$N NMR at natural abundance. J. Magn. Reson. 56:539–542.

Hladky, S. B., and D. A. Haydon. 1972. Ion transfer across lipid membranes in the processes of gramicidin A. I. Studies of the unit conductance channel. Biochim. Biophys. Acta. 274:294–312.

Itoh, M., D. Hagiwara, and T. Kanija. 1975. A new tert-butyloxy-carbonylating reagent, 2-tert-butyloxycarbonyloxyimino-2-phenylacetonitrile. Tetrahedron Lett. 49:4393–4394.

Jordan, P. C. 1984. The total electrostatic potential in a gramicidin channel. J. Membr. Biol. 78:91–102.

Katz, E., and A. L. Demain. 1977. The peptide antibiotics of bacillus: chemistry, biogenesis and possible functions. Bacteriol. Rev. 41:449–474.

Killian, J. A., and B. de Kruijff. 1985a. Thermodynamics, motional, and structural aspects of gramicidin A-induced hexagonal H$_{II}$ phase formation in phosphatidylethanolamine. Biochemistry. 24:7881–7890.

Killian, J. A., and B. de Kruijff. 1985b. Importance of hydration for gramicidin-induced hexagonal H$_{II}$ phase formation in dioleoylphosphatidylcholine model membranes. Biochemistry. 24:7890–7898.

Killian, J. A., F. Borle, B. de Kruijff, and J. Seelig. 1986. Comparative $^2$H and $^{31}$P-NMR study on the properties of palmitoyllysophosphatidylcholine in bilayers with gramicidin A, cholesterol and dipalmitoylphosphatidylcholine. Biochim. Biophys. Acta. 854:133–142.

Kim, K. S., H. L. Nguyen, P. K. Swaminathan, and E. Clementi. 1985. Na$^+$ and K$^+$ ion transport through a solvated gramicidin A transmem-

brane channel: molecular dynamics studies using parallel processors. *J. Chem. Phys.* 89:2870–2876.

Kimball, M. R., and B. A. Wallace. 1984. Crystalline ion complexes of gramicidin A. *Ann. NY Acad. Sci.* 435:551–554.

Koeppe, R. E., and B. P. Schoenborn. 1984. 5-Angstrom fourier map of gramicidin A phased by deuterium-hydrogen solvent difference neutron diffraction. *Biophys. J.* 45:503–507.

Koeppe, R. E., K. O. Hodgson, and L. Stryer. 1978. Helical channels in crystals of gramicidin A and of a caesium-gramicidin A complex: an X-ray diffraction study. *J. Mol. Biol.* 121:41–51.

London, E., and G. W. Feigenson, 1981. Fluorescence quenching in model membranes. An analysis of the local phospholipid environments of diphenylhexatriene and gramicidin A. *Biochim. Biophys. Acta.* 649:89–97.

Mackay, D. H. J., P. H. Berens, K. R. Wilson, and A. T. Hagler. 1984. Structure and dynamics of ion transport through gramicidin A. *Biophys. J.* 46:229–248.

Monoi, H. 1983. Ionic interactions and anion binding in the gramicidin channel. An electrostatic calculation. *J. Theor. Biol.* 102:69–99.

Nabedryk, E., M. P. Gingold, and J. Breton. 1982. Orientation of gramicidin A transmembrane channel: infrared dichroism study of gramicidin in vesicles. *Biophys. J.* 38:234–249.

Naik, V. M., and S. Krimm. 1984. The structure of crystalline and membrane-bound gramicidin A by vibrational analysis. *Biochem. Biophys. Res. Commun.* 125:919–925.

Pines, A., M. C. Gibby, and J. S. Waugh. 1973. Proton enhanced nuclear magnetic resonance of dilute spins in solids. *J. Chem. Phys.* 59:569–590.

Prasad, K. U., T. L. Trapane, D. Busath, G. Szabo, and D. W. Urry. 1982. Synthesis and characterisation of $1$-$^{13}$C-D-Leu$^{12,14}$ gramicidin A. *Int. J. Pept. Protein Res.* 19:162–176.

Prasad, K. U., S. Alonso-Romanowski, C. M. Venkatachalam, L. Trapane, and D. W. Urry. 1986. Synthesis, characterisation and black lipid membrane studies of [7-L-alanine] gramicidin A. *Biochemistry.* 25:456–463.

Rajan, S., S-Y. Kang., H. S. Gutowsky, and E. Oldfield. 1981. Phosphorus nuclear magnetic resonance study of membrane structure. *J. Biol. Chem.* 256:1160–1166.

Rice, D., and E. Oldfield. 1979. Deuterium nuclear magnetic resonance studies of the interaction between dimyristoyl-phosphatidylcholine and gramicidin A. *Biochemistry.* 18:3272–3279.

Sarges, R., and B. Witkop. 1965. Gramicidin V. The structure of valine- and isoleucine-gramicidin A. *J. Am. Chem. Soc.* 87:2011–2020.

Sarin, V. K., S. B. H. Kent, J. P. Tam, and R. B. Merrifield. 1981. Quantitative monitoring of solid-phase peptide synthesis by the ninhydrin reaction. *Anal. Biochem.* 117:147–157.

Smith, R., and B. A. Cornell. 1986. Dynamics of the intrinsic membrane polypeptide gramicidin A in phospholipid bilayers. A solid state $^{13}$C nuclear magnetic resonance study. *Biophys. J.* 49:117–118.

Stark, R. E., L. W. Jelinski, D. J. Ruben, D. A. Torchia, and R. G. Griffin. 1983. $^{13}$C Chemical shift and $^{13}$C-$^{15}$N dipolar tensors for the peptide bond: [1-13C] glycyl[15N]glycine · HCl · H$_2$O. *J. Magn. Reson.* 55:266–273.

Sychev, S. V., and V. T. Ivanov. 1982. Conformational states of gramicidin A in solution and in the membrane. *In* Membranes and Transport. Vol. 2. A. N. Martinosi, editor. Plenum Publishing Corp., New York. 301–307.

Sychev, S. V., and V. T. Ivanov. 1984. Conformations of the transmembrane channel formed by gramicidin A. *Chem. Pept. Proteins.* 2:291–299.

Sychev, S. V., N. A. Neuskaya, ST. Jordoanov, E. N. Shepel, A. I. Miroshnokov, and V. T. Ivanov. 1980. The solution conformations of gramicidin A and its analogues. *Bioorg. Chem.* 9:121–151.

Tanaka, H., and J. H. Freed. 1985. Electron spin resonance studies of lipid-gramicidin interactions utilizing oriented multibilayers. *J. Chem. Phys.* 89:350–360.

Urry, D. W. 1971. The gramicidin A transmembrane channel: a proposed $\pi\pi_{LD}$ helix. *Proc. Natl. Acad. Sci. USA.* 68:672–676.

Urry, D. W. 1984. Ionic mechanisms and selectivity of the gramicidin transmembrane channel: cation nuclear magnetic resonance, dielectric relaxation, carbon-13 nuclear magnetic resonance, and rate theory calculation of single channel currents. *In* Spectroscopy of Biological Molecules. C. Sandorfy and T. Theophanides, editors. D. Reidel Publishing, Dordrecht, Netherlands. 511–538.

Urry, D. W., A. Spisni, and Md. A. Khaled. 1979. Characterization of micellar-packaged gramicidin A channels. *Biochem. Biophys. Res. Commun.* 88:940–949.

Urry, D. W., C. M. Venkatachalam, A. Spisni, R. J. Bradley, R. L. Trapane, and K. U. Prasad. 1980. The malonyl gramicidin channel: NMR-derived rate constants and comparison of calculated and experimental single-channel currents. *J. Membr. Biol.* 55:29–51.

Urry, D. W., J. T. Walker, and T. L. Trapane. 1982. Ion interactions in ($1$-$^{13}$C) D-Val$^8$ and D-Leu$^{14}$ analogues of gramicidin A, the helix sense of the channel and location of ion binding sites. *J. Membr. Biol.* 69:225–231.

Urry, D. W., R. G. Shaw, T. L. Trapane, and K. U. Prasad. 1983*a*. Infrared spectra of the gramicidin A transmembrane channel: The single stranded-B6-helix. *Biochem. Biophys. Res. Commun.* 114:373–379.

Urry, D. W., T. L. Trapane, and K. U. Prasad. 1983*b*. Is the gramicidin A transmembrane channel a single-stranded or double-stranded helix? A simple unequivocal determination. *Science (Wash. DC).* 221:1064–1067.

Van Echteld, C. J. A., R. Van Stigt, B. De Kruijff, J. Leunissen-Bijvelt, A. J. Verkleij, and J. De Gier. 1981. Gramicidin promotes formation of the hexagonal H$_{II}$ phase in aqueous dispersions of phosphatidylethanolamine and phosphatidylcholine. *Biochim. Biophys. Acta.* 648:287–291.

Veatch, W. R., and E. R. Blout. 1974. The aggregation of gramicidin A in solution. *Biochemistry.* 13:5257–5264.

Veatch, W. R., E. T. Fossel, and E. R. Blout. 1974. The conformation of gramicidin A. *Biochemistry.* 13:5249–5256.

Venkatachalam, C. M., and D. W. Urry. 1983. Theoretical conformational analysis of the gramicidin A transmembrane channel. I. Helix sense and energetics of head-to-head dimerisation. *J. Comput. Chem.* 4:461–469.

Wallace, B. A. 1984. Ion-bound forms of the gramicidin A transmembrane channel. *Biophys. J.* 43:114–116.

Wallace, B. A. 1986. Structure of gramicidin A. *Biophys. J.* 49:295–306.

Wallace, B. A., W. R. Veatch, and E. R. Blout. 1981. Conformation of gramicidin A in phospholipid vesicles: circular dichroism studies of effect of ion binding, chemical modification, and lipid structure. *Biochemistry.* 20:5754–5760.

Weinstein, S., B. A. Wallace, E. R. Blout, J. S. Morrow, and W. Veatch. 1979. Conformation of gramicidin A channel in phospholipid vesicles: a $^{13}$C and $^{19}$F nuclear magnetic resonance study. *Proc. Natl. Acad. Sci. USA.* 76:4230–4234.

Weinstein, S., B. A. Wallace, J. S. Morrow, and W. R. Veatch. 1980. Conformation of the gramicidin A transmembrane channel: a $^{13}$C nuclear magnetic resonance study of $^{13}$C-enriched gramicidin in phosphatidylcholine vesicles. *J. Mol. Biol.* 143:1–19.

Weinstein, S., J. T. Durkin, W. R. Veatch, and E. R. Blout. 1985. Conformation of the gramicidin A channel in phospholipid vesicles: a $^{19}$F nuclear magnetic resonance study. *Biochemistry.* 24:4374–4382.